Proceedings of the 6th International Conference on
Computation of Shell and Spatial Structures
IASS-IACM 2008: "Spanning Nano to Mega"
28-31 May 2008, Cornell University, Ithaca, NY, USA
John F. ABEL and J. Robert COOKE (eds.)

Finite element analyses of palm leaf petiole-sheath junctions in simple bending and twisting and in dynamic (oscillatory) flexure

Karl J. NIKLAS*, J. Robert COOKE, Jae Young LEE

*Department of Plant Biology
208 Plant Science Building
Cornell University
kjn2@cornell.edu

Abstract

Finite element analyses were used to estimate qualitatively stress and strain distributions in a stereotypical palm leaf at the petiole-sheath junction when subjected to simple bending and twisting and to simple linear dynamic wind-inducted flexure. This qualitative approach was used because (1) palm leaf morphology and mechanical behavior are unquestionably the most complex in the plant kingdom (e.g., leaf length varies between 0.25 m and 25.1 m), (2) the geometry and material properties of palm leaves vary ontogenetically as well as among different species, and (3) plant morphology and anatomy in general manifests extreme heterogeneity in cross-sectional shape and size and extreme anisotropic material composition. Our analyses reveal heterogeneous stress and strain distributions within the petiole-sheath junction when leaves experience simple bending or twisting and morphological distortions; predicted morphological distortions corresponding to those observed when real palm leaves were bent and twisted. Likewise, simulations of dynamically loaded petiole-sheath junctions reveal strains that are consistent with morphological changes when real leaves are subjected to strong gusts of wind. Finite element analyses indicate that maximum stresses occur in anatomical regions occupied by plant tissues that are strong in tension and relatively extensible compared to neighboring tissues. From these analyses, we conclude that the stereotypical palm leaf base is highly adapted to mechanically support large leaves experiencing large static and dynamic loadings.

1. Introduction

In a seminal paper dealing with the leaf base of palms, Tomlinson wrote ". . . the construction and behavior of the leaf base of palms is [*sic*] a complicated subject which is of considerable morphological interest. It is a problem which can only be understood by considering mechanical aspects of leaf development in relation to the growth of the stem" (Tomlinson, 1962). This assessment remains unchallenged even today. The mechanical behavior and complexity of the palm leaf have no parallels anywhere in the plant kingdom, because in addition to their often great size (which can reach a record length of 25.11 m in the case of *Raphia regalis*), palm leaves possess a tubular leaf sheath (which completely encircles the stem) that supports a cantilevered petiole bearing the leaf lamina (Fig. 1). This tubular sheath, which is anatomically complex owing to a vascular infrastructure of intersecting fibrous strands (Esau, 1967; Gifford and Foster, 1996), persists in some palms as the leaf matures, grows in size, and as the cantilevered petiole bearing the leaf lamina develops (e.g., *Cocos*, *Phoenix*, and *Trachycarpus*). In terms of its biomechanics, the stereotypical palm leaf base normally experiences four kinds of mechanical stresses: stresses resulting from the growth of younger leaves it

Figure 1: Representative palm petiole-sheath junctions. The fleshy tissues of the tubular leaf sheaths of older leaves have broken down to reveal the infrastructures of fibrous vascular strands that provide mechanical support. Younger leaves are enveloped by the sheaths of older leaves.

envelopes, stresses due to the expansion of the stem, and stresses resulting from the weight of the leaf (self-loading), and those resulting from dynamic wind-loading. In addition, the leaf base may experience stresses resulting from the growth of reproductive structures bearing flowers (inflorescences).

Because of this morphological and anatomical complexity, traditional biomechanical analyses of surgically isolated tissues or portions of the palm leaf have been largely uninformative, particularly in helping to evaluate stress-strain distributions in the petiole-sheath junction. To remedy this situation, we used finite element analyses to assess the distribution of the stress magnitudes in this portion of a stereotypical leaf base when it is subjected to simple bending or twisting analyses. We also used this approach to explore the flexural distortions in the petiole-sheath when a leaf is subjected to dynamic wind-induced displacements. Because the size, shape, and tissue material properties of palm leaves change ontogenetically over the course of leaf development and differ among the mature leaves of different species, our analyses necessarily were qualitative rather than quantitative, i.e., we focused on general patterns in stress distributions and gross displacements (stresses). Nevertheless, our analyses point to a number of broad patterns that are consistent with empirical observations and highlight the remarkable functional (adaptive) nature of palm leaf morphology and anisotropic tissue composition.

2. Materials and Methods

2.1 Simple bending and twisting simulations

The nodal displacements were computed by solving the system equations and the strains and stresses were recovered at each integration points using the formulas

$$\varepsilon = \mathbf{B}\Delta \tag{1}$$

$$\sigma = \mathbf{E}\varepsilon \tag{2}$$

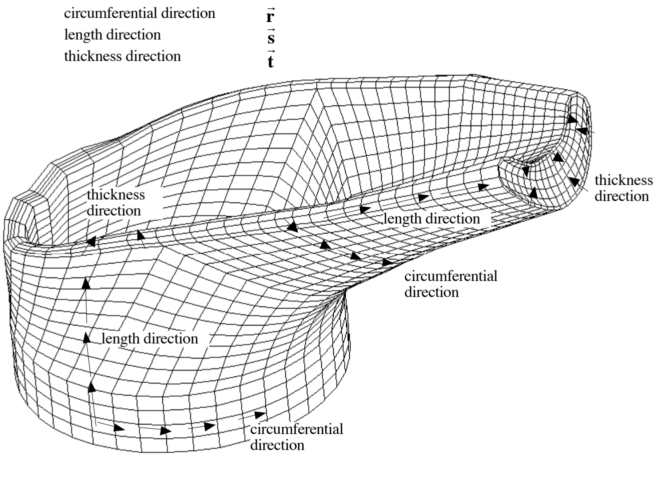

$$E_x = E_L = 5.5\times10^5 psi = 3.78\times10^5 N/cm^2$$
$$E_y = E_R = 2.53\times10^4 psi = 1.74\times10^4 N/cm^2$$
$$E_z = E_T = 8.25\times10^3 psi = 5.68\times10^3 N/cm^2$$
$$\nu_{LR} = 0.229$$
$$\nu_{LT} = 0.488$$
$$\nu_{RT} = 0.665(0.465)$$
$$\nu_{TR} = 0.217(0.152)$$
$$\nu_{RL} = 0.011$$
$$\nu_{TL} = 0.007$$
$$E_{inside} = 5\times10^3 N/cm^2$$
$$\nu_{inside} = 0.5$$

Figure 2. Mesh and anisotropic properties used ***NOTE:*** *See the Extended Abstract CD for enlarged figures.*

Figure 2 lists the numerical values used to evaluate the stresses and strains. However, it is important to note that our analyses provide only qualitative assessments of stress and strain distributions because the foregoing numerical values are simply indicative, and do not apply to all palm species.

2.2 Dynamic simulations

Dynamic equilibrium equation

$$\mathbf{M}\ddot{\Delta} + \mathbf{C}\dot{\Delta} + \mathbf{K}\Delta = \mathbf{F} \tag{3}$$

where $\mathbf{M}$=mass matrix, $\mathbf{C}$=damping matrix, $\mathbf{K}$=stiffness matrix, $\mathbf{F}$=force vector, $\ddot{\Delta}$=acceleration, $\dot{\Delta}$=velocity, and Δ=displacement.

The vibration modes are extracted by solving the eigenvalue problem

$$\mathbf{M}\ddot{\Delta} + \mathbf{K}\Delta = 0 \tag{4}$$

for free vibrations without damping and external forces. The square roots of eigenvalues represent the frequency of vibration (radian/sec), and corresponding eigenvectors represent the vibration mode shapes. The nodal displacements at a given time step is computed by linear combination of the vibration mode shapes.

In our analysis, the mode superposition method was applied with Newmark integration scheme. The eigenvalues are extracted from the smallest value, i.e., lowest frequency. The modes with lower frequency usually have more effect to the dynamic motion than those with higher frequency. Only the lowest 7 modes were used in the analysis, because the rest of the modes were assessed to have insignificant effects.

3. Results

3.1 Simple bending and twisting simulations

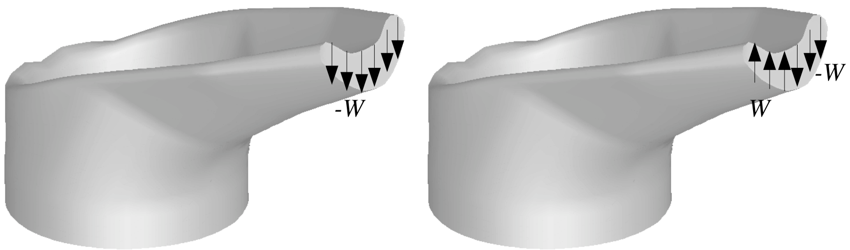

Figure 3. Simple bending (left) and twisting (right) loading

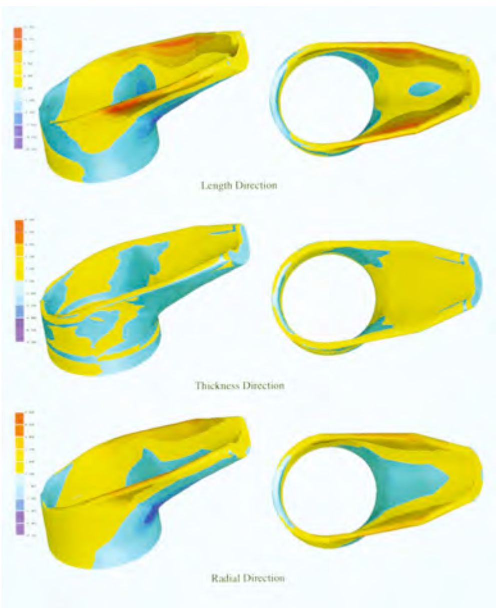

Figure 4: A finite element predicted stress distributions for a stereotypical palm leaf petiole (at right)-sheath (left) junction subjected to **simple bending**.
Top: Length direction; middle: thickness direction; bottom: radial direction

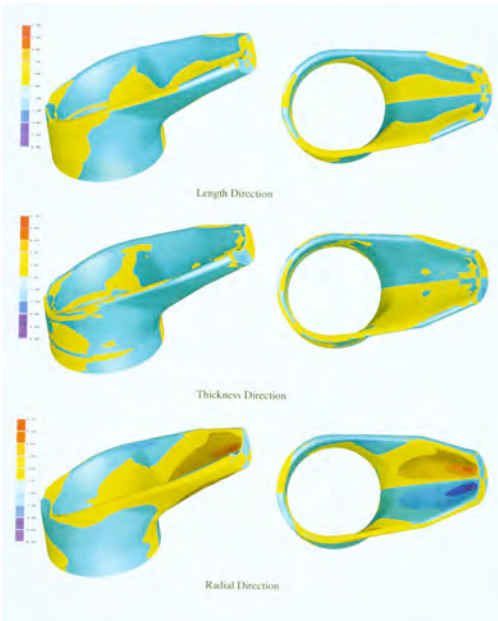

Figure 5: A finite element predicted stress distributions for a stereotypical palm leaf petiole (at right)-sheath (left) junction subjected to **twisting.**
Top: Length direction; middle: thickness direction; bottom: radial direction

3.2 Dynamic wind-induced flexure simulations

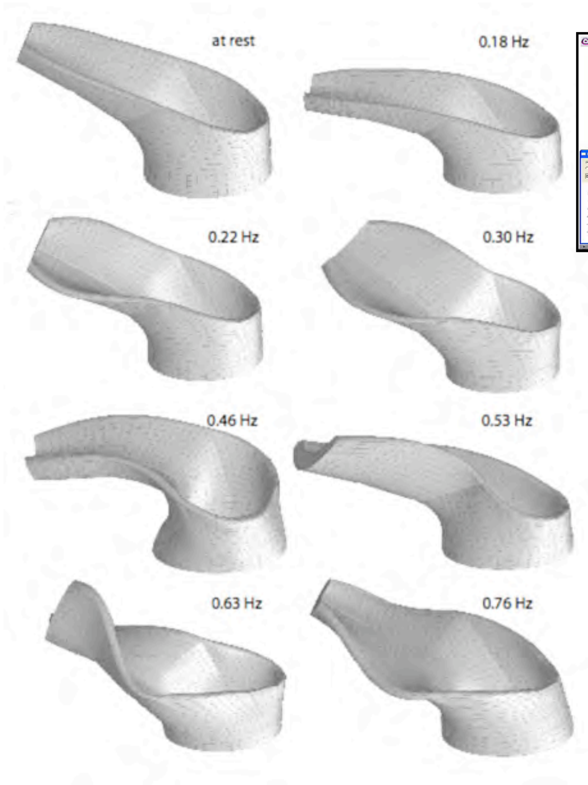

Figure 6: Seven lowest modal shapes for a stereotypical palm leaf petiole (at right)-sheath (left) junction.

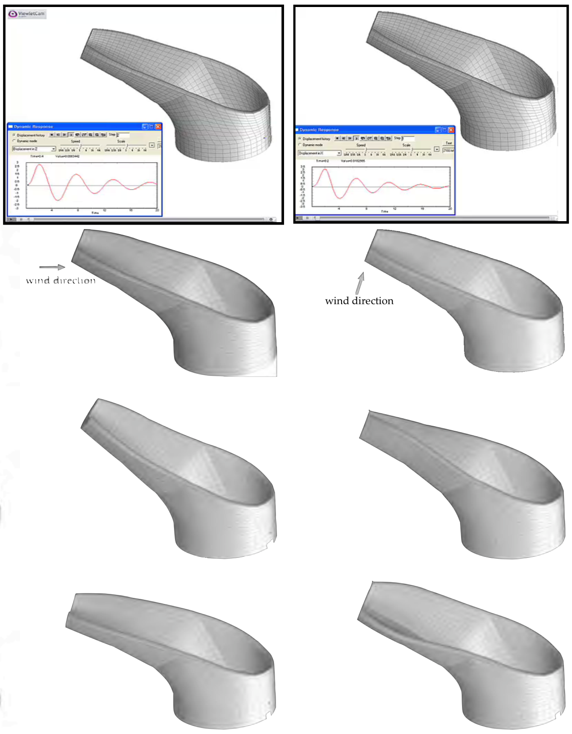

Figure 7: Transient: Left column (wind horizontal: middle max; bottom min); right column (wind upward: middle at max; bottom at minimum). Double-click the top row of images for animations.

Figure 6 displays the mode shapes for the seven lowest natural frequencies because the rest of the modes turned out to have an insignificant effect. The modes with lower frequency usually have more effect to the dynamic motion than those with higher frequency. Figure 7 shows snapshots of the response to a single half-sine-wave when directed horizontally (left column) and upward (right column).

NOTE: Flash animations (.SWF and .MOV files) of wind-induced transient oscillations are contained in the CD version of this abstract. The embedded .mov files require that a QuickTime player be installed.

References

[1] Hughes TJR. The Finite Element Method: Linear Static and Dynamic Finite Element Analysis (2nd edn). Dover, 2000.

[2] Simo JC and Armero F. Geometrically non-linear enhanced strain mixed methods and the method of incompatible modes. *International Journal for Numerical Methods in Engineering* 1992; **33**:1413-1449.

[3] Wilson EL, Taylor RL, Doherty WP, Ghaboussi J. Incompatible displacement models. In *Numerical and Computer Models in Structural Mechanics*, Robinson AR, Fenves SJ, Perrone N, Schnobrich WC (eds). Academic Press: New York, 1973; 43-57.